

BIROn - Birkbeck Institutional Research Online

Bhatti, M. and McHugh, T. and Milanesi, Lilia and Tomas, Salvador (2014) Self-assembled nanoparticles as multifunctional drugs for anti-microbial therapies. *Chemical Communications* 50 , pp. 7649-7651. ISSN 1359-7345.

Downloaded from: <https://eprints.bbk.ac.uk/id/eprint/9787/>

Usage Guidelines:

Please refer to usage guidelines at <https://eprints.bbk.ac.uk/policies.html>
contact lib-eprints@bbk.ac.uk.

or alternatively

COMMUNICATION

Self-assembled nanoparticles as multifunctional drugs for anti-microbial therapies

Cite this: DOI: 10.1039/x0xx00000x

Manpreet Bhatti,^{*, a} Timothy D. McHugh,^b Lilia Milanese,^c and Salvador Tomas^{*, a}

Received 00th January 2012,

Accepted 00th January 2012

DOI: 10.1039/x0xx00000x

www.rsc.org/

A self-assembled nanoparticle containing a photosensitizer and a Trojan-horse moiety (cholesterol), binds an anti-TB pro-drug and increases 1000-fold its activity against mycobacteria. These minimalist constructs will allow development of economically viable, efficient drug preparations for the treatment of drug-resistant TB infections.

The recent UK Chief Medical Officers report has emphasized the increasing threat of antimicrobial resistance and the need for new strategies for control.^{1,2} This is particularly true for tuberculosis (TB). TB accounts for around 9 million new cases a year globally and 1.4 million deaths.³ This fact is compounded by over half a million cases of multi drug resistant (MDR) and extreme drug resistant (XDR) TB per year. The options for treating TB are limited, the drugs in the approved regimens were introduced in the 1960's and new moieties are still in early phase testing. The cause for concern is that the new compounds are focused on limited targets and so cross-resistance is a real risk.⁴ Clearly, new paradigms for antimicrobial delivery are required. One such paradigm may rest in the development of soft nanoparticles as vehicles for targeted and controlled delivery

In the last years the development of antimicrobials based on nanoparticles has attracted strong interest.^{5,6} For the treatment of *Mycobacterium tuberculosis* specifically, studies have so far focused on the sustained drug delivery properties of relatively simple nanoparticle preparations (mostly solid lipid and polymer based), using traditional drugs.^{7,8} However nanoparticle assemblies offer the possibility of introducing functionality beyond the passive release of the drug.^{9,10} The level of sophistication that can potentially be reached is illustrated by the "artificial organelle" approach.¹¹ These approaches, although potentially very efficient, are expensive to develop and produce. On the other hand, a nanoparticle can be produced that is formed exclusively of small, uncomplicated molecules, each one with different functionality, but with an overall therapeutic effect that is larger than the sum of the individual parts. Here we develop a multifunctional nanoparticle that can be potentially applied to the treatment of TB. The nanoparticle will contain bacterial nutrient, a photosensitizer (PS) for photodynamic therapy (PDT) and an anti-TB drug. In PDT, a PS is activated by

light of an appropriate wavelength producing reactive oxygen species that cause cell death. PDT is being used for cancer treatment,¹² but its application to bacterial infections has been so far limited.^{13,14}

Recently, we described the synthesis and molecular recognition properties of very stable (CMC 11 nM), hydrophobically self-assembled nanoparticles based on a Zn-metalloporphyrin amphiphile that contained also cholesterol.¹⁵ We reasoned that nanoparticles based on this design can be used for the targeted delivery of drugs that bind to the nanoparticle. Additionally, the chemistry of the amphiphile can be tailored in order to introduce targeting and enhance transport and towards photodynamic therapy (PDT) applications.¹⁶ For the development of an agent for the treatment of mycobacterium infections, we used the same amphiphilic building block as earlier described, but introduced Co instead of Zn as the metal centre, leading to amphiphile **1** (Fig. 1, Supplementary Fig. 1).

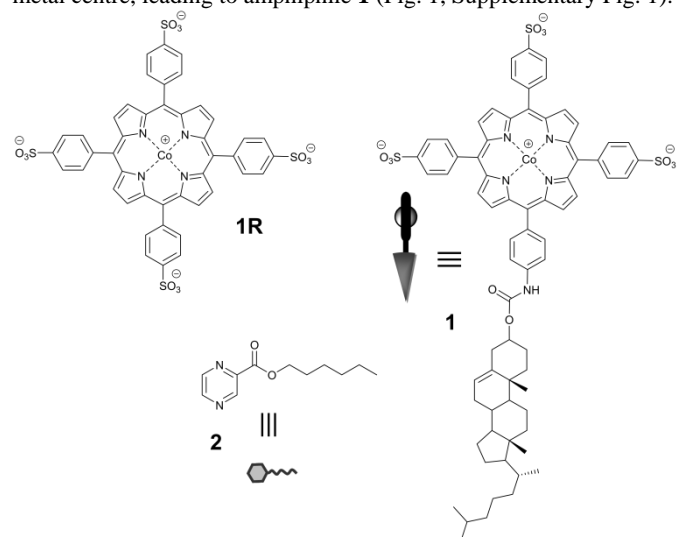


Figure 1. Chemical structure of water soluble porphyrin **1R**, amphiphilic porphyrin **1** and pyrazinoic acid ester **2**, together with their cartoon representations

It is known that mycobacteria are capable of using cholesterol as an important carbon source during infections and during growth in culture¹⁷ therefore, the presence of the cholesterol in the molecule is expected to provide some degree of targeting and facilitate the transport inside the bacterium. Co was chosen as the porphyrin metal centre for two reasons. First, Co metalloporphyrins are likely to be more efficient photosensitizers than Zn metalloporphyrins as they quench oxygen at a slower rate than Zn metalloporphyrins,¹⁶ rendering a Co-porphyrin derivative a (potentially) better PDT agent. Second, Co-metalloporphyrins have a stronger affinity for N basic-bearing ligands than the Zn counterparts, which will make it a more efficient molecular receptor to our drug model and potentially enhance its transport. A version of **1**, unable to form nanoparticles, **1R**, was also synthesized for comparison purposes (Fig. 1, Supplementary Fig. 2). As a drug model we synthesized a hydrophobic pyrazinoic acid derivative, pyrazinoic acid hexylester **2**, by treatment of pyrazinoic acid with oxalyl chloride followed by addition of hexanol (Fig. 1, Supplementary Fig. 3)

While pyrazinoic acid is the active form of the drug,¹⁸ pyrazinoic acid ester **2** was selected because its hydrophobicity should make it bind more strongly to the nanoparticle than the free acid, and because ester moieties hydrolyze slowly but spontaneously in water, while amides typically require enzymatic assistance for the hydrolysis to take place in measurable timescales.¹⁹ This may lead to bacterial resistance as demonstrated by mycobacterium resistance to the prodrug pyrazinamide.²⁰

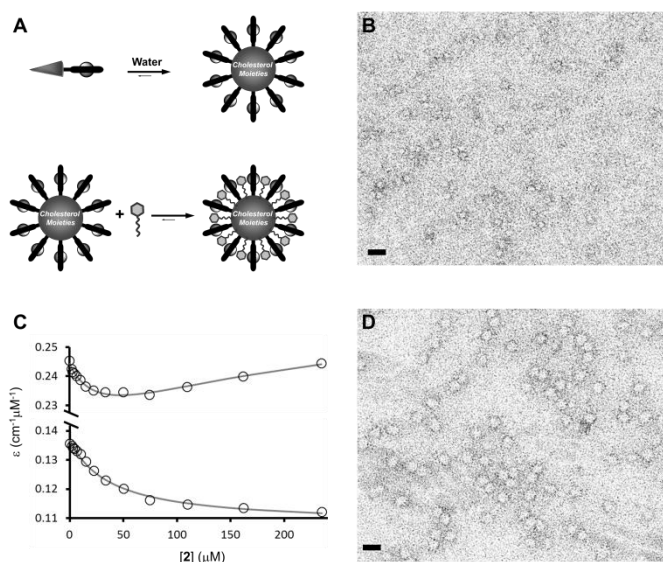


Figure 2. A. Cartoon representation of the nanoparticle assembly and the formation of the complex nanoparticle-ester **2**. B. TEM picture (negative stain) of **1** nanoparticles in the working buffer. The scale bar represents 20 nm. C. Variation of the extinction coefficient of a solution of nanoparticles upon addition of ester **2** (empty circles). The fitting to a binding model for the sequential binding of two **2** molecules per molecule of **1** is shown as a line for changes at 428 nm (upper curve) and at 415 nm (lower curve). See Supplementary Table 1 for K_{app} values and Supplementary Fig. 4B for limiting values of extinction coefficients. D. TEM picture (negative stain) of the nanoparticles in presence of **2**. The scale bar represents 20 nm

Amphiphilic porphyrin **1** assembles into a nanoparticle of similar size and appearance to that of the previously described Zn derivative¹⁵ (Fig. 2A and 2B). The apparent binding affinity of

pyrazinoic acid and the ester **2** with **1** was determined by means of UV titration experiments (Fig. 2C, Supplementary Fig. 4). The binding isotherm is consistent with the sequential binding of two molecules of **2** for each molecule of receptor **1**. This result is in agreement with literature data on complexation of Co metalloporphyrins with amines, which show that the metal centre can bind two ligands.²¹ The apparent binding constants are 3.4×10^4 M⁻¹ and 4.5×10^3 M⁻¹ for the first and second binding event respectively (see Materials and Methods section for details and Supplementary Table 1). In contrast, the binding of **2** to a cobalt porphyrin receptor that does not form nanoparticles show binding constants of 4.5×10^3 M⁻¹ for the first binding event and 50 M⁻¹ for the second (see Supplementary Table 1). Moreover, for the nanoparticle, but not for **1R**, the ligand may also bind in a non-specific manner (yielding complexes with stoichiometry larger than 1:2) via insertion of the hydrophobic tail. The implications are that, upon de-assembly of the particle (for example, as the cholesterol moiety is metabolized into the bacteria), the drug will be more easily released. TEM pictures of **1** shows that the ligand increases the size of the nanoparticles from an average 9.5 to 12.3 nm diameter in presence of **2** (Figs. 2 B and D), consistent with ligand binding to the nanoparticle.

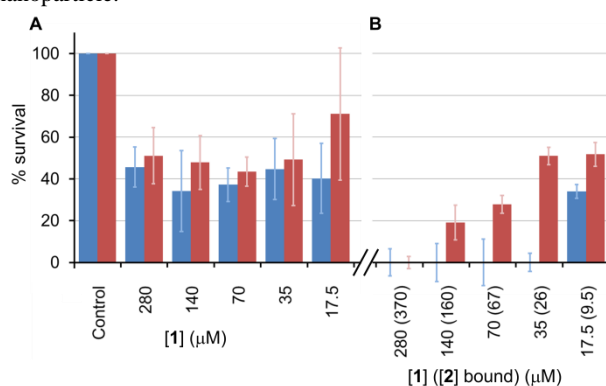


Figure 3. A. Percentage survival of *M. fortuitum* 4 days after treatment with pure **1**. Red columns represent the survival for non-irradiated samples and the blue columns the survival for samples that were irradiated 24 hours after exposure to the nanoparticle (75 J/cm² energy dose). B. Idem for samples treated with **1** and **2**. The ratio of concentrations [2]:[1] is 2 in all samples. The concentration of **2** bound to the nanoparticle is shown in parenthesis and has been calculated from the binding constants. See Supplementary Table 2 and 3 for numerical data. In all cases, the error bars represent twice the standard deviation of three measurements.

Mycobacterium fortuitum was chosen as a model for *in vitro* bacteria killing experiments. *M. fortuitum* is a fast growing mycobacterium that can be manipulated under containment level 2 conditions making it a useful surrogate for *M. tuberculosis*.²² *M. fortuitum* was treated either with nanoparticle **1**, ester **2** or nanoparticle **1** in presence of **2**, at a molar ratio 2:1 drug **2**/receptor **1** (see Supplementary Information for details). For *M. fortuitum* treated with **2** alone, a concentration up to 50 mM (8.6 mg/mL) is required for bacterial cell death under the conditions used in this study. Below these concentrations the drug does not show any effect. For these experiments, the addition of water soluble porphyrin **1R** up to 280 μM did not have any effect on the cell survival. For nanoparticle **1** alone, the bacterium survival is around 40-50% when the concentration of the nanoparticle 35 μM, going up to 60% when the concentration is further lowered to 17.5 μM. (Fig. 3A, Supplementary Table 2)

Irradiation of the samples with light at 430 nm (the maximum absorption of the nanoparticle) results on a decrease in survival of 10-15 % in relation to not irradiated samples for all the concentrations tested (Fig. 3A, Supplementary Table 2). This result is attributed to the photosensitizer action of the metalloporphyrin moiety within the bacteria upon irradiation. When treated with nanoparticle **1** in the presence of **2**, quantitative killing takes place for samples 280 μM in **1** (with 370 μM of **2** bound to nanoparticle), while the survival of bacterium increases in a typical dose-dependent fashion as the concentrations tested decrease, up to 50% survival for samples with 17.5 μM in **1** (with 9.5 μM of **2** bound to nanoparticle). (Fig.3B, Supplementary Table 3). Finally, when samples treated with **1** in presence of **2** are also irradiated at 430 nm quantitative killing takes place down to concentrations of **1** 35 μM (with 26 μM of **2** bound to nanoparticle), while a survival of 40% approx. is observed when the concentration is further lowered to 17.5 μM in **1** (with 9.5 μM of **2** bound to nanoparticle). This result is consistent with the nanoparticle facilitating the transport of the pyrazinoic acid ester **2**, together with the expected photosensitizer action of the porphyrin moiety

Conclusions

In summary, this work shows that the combination of a small molecule based nanoparticle (**1**) with the appropriate derivative of a known drug (**2**) results in quantitative bacterial killing for *M. fortuitum*, a widely used model for *M. tuberculosis* down to 15 $\mu\text{g}/\text{mL}$ from 10 mg/mL for the drug **2** in absence of the nanoparticle (Fig. 3, Supplementary Tables 2 and 3). The enhancing of the drug activity in the presence of the nanoparticle is attributed to the ability of the nanoparticle to facilitate the transport of the drug into the bacteria and is supported by the fact that the nanoparticle on its own leads to bacterial killing upon irradiation. The transport activity can be attributed to the presence of a cholesterol moiety. Cholesterol is used by *M. fortuitum* as nutrient enabling the transport of the other moieties associated to it, such as drug model **2** and the covalently linked Co metalloporphyrin moiety. It is also possible that the nanoparticle components de-assemble when in contact with the bacterial cell wall and incorporate as individual molecules. Irradiation may then lead to bacterial wall damage resulting in enhanced drug absorption. Whatever the precise mechanism of action, these kinds of nanoparticles are a strong candidate to be developed into therapeutic agents for resilient strains of tuberculosis that currently require drastic treatment, including pulmonary surgery.²³ A combined therapy based on the use of a system such as the one described here will offer a much more convenient alternative, both from the patient and the economic point of view. The use of UV to enhance drug activity will not be practical in most patients. However, in those with MDR and XDR TB, where treatment options are limited, use of an adapted bronchoscope could provide targeted UV delivery to the site of disease. The modular nature of the nanoparticles and the relative simplicity of the building blocks should allow us to develop related systems with different properties. For example, a version bearing ergosterol may target fungi²⁴ and can be tested against post-transplant fungal infections. The potential toxicity of our porphyrin derivatives

may be mitigated by developing a nanoparticle version bearing more biocompatible (e.g. heme derivative) moieties. The potential of these systems is currently being analysed in our labs.

Notes and references

^a Institute of Structural and Molecular Biology and Department of Biological Sciences, School of Science, Birkbeck, University of London, Malet Street. London WC1E 7HX, UK.

e-mail: s.tomas@bbk.ac.uk and m.bhatti@ucl.ac.uk.

^b Centre for Clinical Microbiology, Royal Free Campus, University College London, Rowland Hill Street, London NW3 2QG, UK.

^c School of Biological and Chemical Sciences, Queen Mary, University of London, Mile End Road, London E1 4NS, UK.

Electronic Supplementary Information (ESI) available: General experimental methods, synthesis and characterization of **1** and **2**, binding constants measurements, TEM experimental details and detailed microbiology experiments.. See DOI: 10.1039/c000000x/

- 1 S. C. Davies, *Annual Report of the Chief Medical Officer*, 2011, **2**.
- 2 Infections and the rise of antimicrobial resistance *London: Department of Health*, 2013.
- 3 *World Health Organisation World tuberculosis report*, 2012. http://apps.who.int/iris/bitstream/10665/91355/1/9789241564656_en_g.pdf.
- 4 A. S. Ginsburg, J. H. Grosset, W. R. Bishai, *Lancet Infect. Dis.*, 2003, **3**, 432.
- 5 A. J. Huh, Y. J. Kwon, *J. Control. Release*, 2011, **156**, 128.
- 6 A. C. Engler, N. Wiradharma, Z. Y. Ong, D. J. Coady, J. L. Hedrick, Y. Y. Yang, *Nano Today* 2012, **7**, 201.
- 7 J. C. Sung, D. J. Padilla, L. Garcia-Contreras, J. L. VerBerkmoes, D. Durbin, C. A. Peloquin, K. J. Elbert, A. J. Hickey, D. A. Edwards, *Pharm. Res.*, 2009, **26**, 1847.
- 8 A. Sosnik, A. M. Carcaboso, R. J. Glisoni, M. A. Moreton, D. A. Chiappetta, *Adv. Drug Deliv. Rev.*, 2010, **62**, 547.
- 9 M. H. Xiong, Y. Bao, X. Z. Yang, Y. C. Wang, B. Sun, J. Wang, *J. Am. Chem. Soc.*, 2012, **134**, 4355.
- 10 A. F. Radovic-Moreno, T. K. Lu, V. A. Puscasu, C. J. Yoon, R. Langer, O. C. Farokhzad, *ACS Nano*, 2012, **6**, 4279.
- 11 P. Tanner, P. Baumann, R. Enea, O. Onaca, C. Palivan, W. Meier, *Acc. Chem. Res.*, 2011, **44**, 1039.
- 12 D. Fayter, M. Corbett, M. Heirs, D. Fox, A. Eastwood, *Health Technol. Assess.*, 2010, **14**, 1.
- 13 G. B. Kharkwal, S. K. Sharma, Y. Y. Huang, D. Tianhong, M. R. Hamblin, *Lasers Surg. Med.* 2011, **43**, 755.
- 14 K. O'Riordan, D. S. Sharlin, J. Gross, S. Chang, D. Errabelli, O. E. Akilov, S. Kosaka, G. J. Nau, T. Hasan, *Antimicrob. Agents Chemother.*, 2006, **50**, 1828.
- 15 S. Tomas, L. Milanesi, *J. Am. Chem. Soc.*, 2009, **131**, 6618.
- 16 R. Bonnet, G. Martinez, *Tetrahedron*, 2001, **57**, 9513.
- 17 A. Brzostek, J. Pawelczyk, J. Dziadek, *J. Bacteriol.*, 2009, **191**, 6584.
- 18 Y. Zhang, D. Mitchison, *Int. J. Tubercul. Lung. Dis.*, 2003, **7**, 6.
- 19 M. F. Simoes, E. Valente, M. J. Gomez, E. Anes, L. Constanito, *Eur. J. Pharm. Sci.*, 2009, **37**, 257.
- 20 J. K. McClatchy, A. Y. Tsang, M. S. Cernich, *Antimicrob. Agents. Chemother.*, 1982, **20**, 556.
- 21 U. Michelsen, C. A. Hunter, *Angew. Chem. Int. Ed.*, 2000, **39**, 764.

- 22 A. Gupta, S. J. Bhakta, *Microb. Chemother.*, 2012, **67**, 1380.
- 23 L. Bertolaccini, A. Viti, D. P. Giovanni, A. J. Terzi, *Thorac. Dis.*, 2013, **5**, 198.
- 24 R. J. Kieber, W. J. Payne, G. S. Appleton, *Appl. Microbiol.*, 1955, **3**, 247.